Stereocomplexation of Stereoregular Aliphatic Polyesters: Change from Amorphous to Semi-Crystalline Polymers with Single Stereocenter Inversion

Yanay Popowski,[‡,†] Yiye Lu,[‡,‡] Geoffrey W. Coates,*[,‡] and William B. Tolman*[,†]

[†] Department of Chemistry, Washington University in St. Louis, One Brookings Hall, Campus Box 1134, St. Louis, MO 63130-4899, United States of America

[‡] Department of Chemistry and Chemical Biology, Baker Laboratory, Cornell University, Ithaca, New York 14853-1301, United States of America

ABSTRACT: Stereocomplexation is a useful strategy for the enhancement of polymer properties by the co-crystallization of polymer strands with opposed chirality. Yet, with the exception of PLA, stereocomplexes of biodegradable polyesters are relatively underexplored and the relationship between polymer microstructure and stereocomplexation remains to be delineated, especially for copolymers comprised from two different chiral monomers. In this work, we resolved the two enantiomers of a non-symmetric chiral anhydride (CPCA) and prepared a series of polyesters from different combinations of racemic and enantiopure epoxides and anhydrides, via metal-catalyzed ring-opening copolymerization (ROCOP). Intriguingly, we found that only specific chiral combinations between the epoxide and anhydride building blocks result in the formation of semicrystalline polymers, with a single stereocenter inversion inducing a change from amorphous to semicrystalline copolymers. Stereocomplexes of the latter were prepared by mixing an equimolar amount of the two enantiomeric copolymers, yielding materials with increased melting temperatures (ca. 20 °C higher) compared to their enantiopure constituents. Following polymer structure optimization, the stereocomplex of one specific copolymer combination exhibits a particularly high melting temperature (T_m = 238 °C).

Introduction

The replacement of commodity plastics by bio-derived and environmentally benign alternatives is an ongoing endeavor owing to the environmental toll imposed by traditional polymers derived from fossil fuels.[1] Aliphatic polyesters, such as polyhydroxyalkanoates (PHAs) and polylactic acid (PLA), are notable targets owing to the hydrolytically susceptible ester linkage in their backbone and their bio-compatibility.[2,3] Such polymers typically are derived from a single monomer, but this sourcing narrows the possibilities for tuning of their thermal and physical properties.[4] The metal-catalyzed ring-opening copolymerization (ROCOP) of epoxides and cyclic anhydrides, two building blocks that may be structurally varied, has emerged as an alternative, powerful tool for the preparation of polyesters.[5,6] Providing versatility in structure and property design, ROCOP has been used to prepare aliphatic polyesters from renewable resources with competitive properties relative to aromatic polyesters.[7-9] To further improve the polymer performance, monomer structure, polymer stereochemistry, and polymer architecture also have been investigated.[10]

High stereoregularity in the polymer backbone often leads to enhanced properties.[11] In addition to cases where high tacticity or enantipurity orders packing of polymer chains, such ordering can also occur upon co-crystallization and assembly of two enantiopure polymers with opposite chirality (stereocomplexation), with the resulting crystallinity reflected in an increase in the melting temperature (T_m).[10,12,13] Stereocomplexation has been found to be a useful strategy for enhancing polymer thermal properties beyond those of its enantiopure constituents, with the effects being dependent on the structural attributes of the monomeric units. PLA-related polymers have been studied extensively for stereocomplexation,[14-16] and other examples include polymethylmethacrylates,[17-22] polycarbonates,[12,23-29] polyhydroxyalkanoates,[30-32] polysaccharides,[33] and polycarbodiimides.[34] Notwithstanding these advances, the number of polyester stereocomplexes is modest and much remains to be learned about the factors contributing to stereocomplexation.[35-45]

A key research goal is to elucidate the stereochemical enhancement of aliphatic polyester properties and expand the scope of possible stereocomplexes in order to access new and potentially useful properties (Scheme 1).[46] In previous work, the synthesis of stereoregular poly(propylene succinate) by ROCOP using enantiopure propylene oxide (PO) was reported, and its corresponding stereocomplex was prepared by mixing equimolar amounts of the enantiopure isotactic *R* and *S* polymers. An increase in the T_m of nearly 40 °C was observed upon stereocomplexation ($T_{m,sc}$ = 120 °C) of the homochiral copolymers.[47] The chiral salcy-Co catalyst used afforded high regiocontrol in the enchainment of the asymmetric

Scheme 1. Regioregular polyester stereocomplexes.

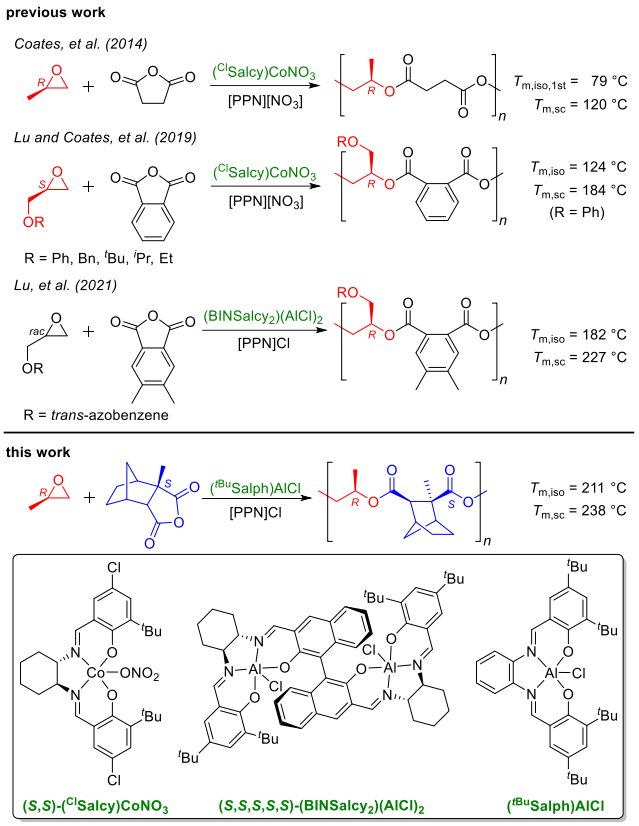

epoxides, which also was beneficial in the preparation of a series of stereoregular aromatic polyesters. These latter copolymers, prepared by ROCOP of phenyl glycidyl ethers and benzoic anhydride, also were shown to undergo stereocomplexation, thanks to the rigid backbone phenyl ring.[48] More recently, a BINOL-based chiral salcy-Al catalyst demonstrated both high regio- and stereocontrol in ROCOP of *racemic* or *meso* epoxides with cyclic anhydrides. The resulting polymers also exhibited stereocomplexation, with an increase of between 25–45 °C in the T_m compared to the enantiopure constituents.[49,50] In all of the aforementioned work, the regiocontrol was only achieved with the asymmetric epoxides, leaving the asymmetric anhydride regiocontrol unexplored. Furthermore, the stereoregularity of the polymers was derived from the inherent chirality of a single building block (epoxide), whereas the role of complemental chirality of two building blocks (epoxide and anhydride) and its effect on polymer properties was not investigated. Studies of stereospecificity in anhydride ring-opening have been limited to the symmetric carbic anhydride (CPMA) and maleic anhydride (MA), focusing on differences in backbone microstructures derived from *endo*- or *exo*-CPMA and *cis*- or *trans*-MA.[51-55] These reports only offered partial insight into the relationship between microstructures and polymer properties, stereocomplexation was not described, and further studies were limited by post-polymerization epimerization.

We therefore sought to prepare and investigate the stereoselective interactions between polyesters comprised of both enantiomerically-pure epoxide and anhydride building blocks. Inspired by previously reported regioselective ROCOP processes with bio-sourced anhydrides using an achiral salph-Al catalyst,[56] we chose to copolymerize butylene oxide (BO) and PO with 2-methyl-5-norbornene-2,3-dicarboxylic anhydride (CPCA), the Diels–Alder adduct of cyclopentadiene and citraconic anhydride, as a model non-symmetric anhydride. The latter is an isomerized product of itaconic anhydride, which is derived from citric acid pyrolysis or itaconic acid dehydration, with both acids readily available from biomass fermentation.[57-59] We report the discovery of copolymers of CPCA and PO that with specific stereoisomer combinations form stereocomplexes having high melting temperatures, with a T_m as high as 240 °C attainable upon optimization of the polymer structure.

Scheme 2. Synthesis of CPCA enantiomers.

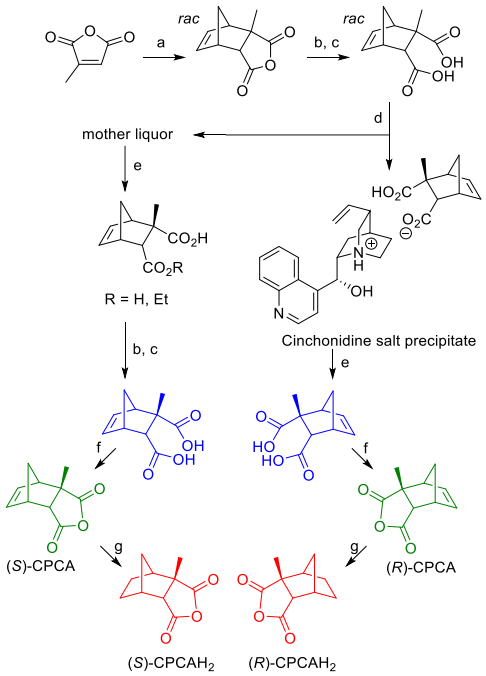

Conditions: a) Cyclopentadiene, $CHCl_3$, R.T., 24 h; b) $NaOH_{(aq)}$ 4 M, 80 °C, 2 h; c) 37% HCl, R.T., 1 h; d) Cinchonidine, 85% EtOH, 90 °C; e) 10% HBr, R.T.; f) AcCl, reflux, 30 min; g) 10% Pd/C, R.T., 24 h.

Results and Discussion

To synthesize polyesters derived from optically-pure anhydrides, we first resolved the two enantiomers of CPCA, which were prepared by the Diels–Alder cycloaddition of cyclopentadiene and citraconic anhydride (Scheme 2). After hydrolyzing the racemic cyclic anhydride (CPCA; 25 g) to the corresponding diacid under basic conditions (89% yield; b and c), the (*R*)-enantiomer was selectively crystalized in high yield as a mono-salt by treatment with the enantiopure natural base cinchonidine (27 g, 88% yield; d).[60] The (*R*)-diacid was restored upon treatment with HBr and converted back to the anhydride with acetyl chloride, affording the (*R*)-CPCA enantiomer in a multi-gram scale and in high yield (6.1 g, 86% overall yield; e and f). The (*S*)-CPCA anhydride was isolated by treating the mother liquor of the (*R*)-CPCA crystallization with HBr and hydrolyzing the obtained (*S*)-CPCA diacid and corresponding ethyl ester mixture with 4M NaOH (18 g, 81% yield; e, b and c).

Table 1. Polymerization conditions and characterizations of poly(BO-*alt*-CPCA) and poly(PO-*alt*-CPCA)

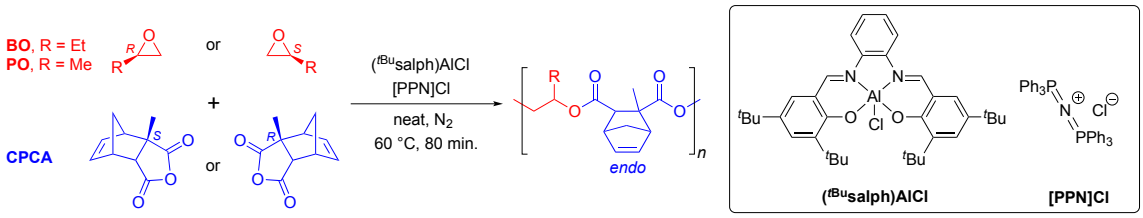

entry[a]	epoxide	epoxide/CPCA	$M_{n\,GPC}$ (kDa)[b]	$Đ$ (M_w/M_n)[b]	T_g (°C)[c]	T_m (°C)[c] 1st heat	T_m (°C)[c] 2nd heat	T_c (°C)[c]
1	BO	*R*/*R*	6.7	1.08	51	n.d.	n.d.	n.d.
2	BO	*S*/*R*	8.1	1.10	52	156	n.d.	n.d.
3	BO	*R*/*R* + *S*/*S*[d]	5.9	1.09	51	n.d.	n.d.	n.d.
4	BO	*S*/*R* + *R*/*S*[d]	7.1	1.10	55	150, 166	n.d.	n.d.
5	PO	*R*/*R*	8.1	1.11	69	n.d.	n.d.	n.d.
6	PO	*S*/*R*	5.9	1.16	57	191	183	157
7	PO	*R*/*R* + *S*/*S*[d]	6.9	1.18	61	n.d.	n.d.	n.d.
8	PO	*S*/*R* + *R*/*S*[d]	–[e]	–[e]	58	218	216	173

[a] [epoxide]:[CPCA]:[cat.]:[PPNCl] = 500:100:1:1. [epoxide] = 3.8 mmol. [b] Determined by GPC in THF, calibrated with polystyrene standards. [c] Determined by DSC. Reported T_g values are from second heat, T_m values are from first heat and second heat, and T_c values are from the first cool. [d] 1:1 mixture of enantiomeric polymers. [e] Not determined due to poor solubility. n.d. = none detected.

Subsequently, conversion of the diacid to the cyclic anhydride, as described for the (*R*)-CPCA enantiomer, provided (*S*)-CPCA in a corresponding yield. Chiral High-Performance Liquid Chromatography (HPLC) was used to evaluate the enantiopurity of the CPCA monomers. By comparing the retention times to those observed for the enantiomers of *rac*-CPCA, we determined that both anhydrides were obtained in high enantiopurity, 97–99% and 99% for (*R*)-CPCA and (*S*)-CPCA, respectively (see electronic supporting information; Figure S1).

A series of regioregular poly(BO-*alt*-CPCA) and poly(PO-*alt*-CPCA) polyesters was prepared by employing either racemic or enantiopure building blocks and a binary catalytic system comprising of [PPN]Cl and (*t*Busalph)AlCl, a highly regioselective catalyst for the copolymerization of epoxides and anhydrides (Table 1 and Table S1).[56,61] The polymerizations were performed in neat epoxide and stopped shortly after reaching complete anhydride conversion in order to avoid undesired epimerization and transesterification side reactions (80 min.; determined by the typical color change of the reaction to red and corroborated by ^{1}H NMR spectroscopy).[61,62] The polymers were precipitated by the addition of methanol to the dichloromethane (DCM) product solution and dried under vacuum, resulting in high isolated yields (typically between 90–95%). The number-average molecular weight (M_n) of the polyesters ranged between 5.6 and 10.9 kDa. Well-controlled polymerization processes were evidenced by low dispersity values ($Đ \sim 1.1$).

The microstructures of the resultant polyesters were analyzed by ^{1}H and ^{13}C{^{1}H} NMR spectroscopy. For example, the NMR stack plot in Figure 1 enables comparison of the microstructures of a series of poly(BO-*alt*-CPCA) copolymers prepared with both enantiomerically-pure epoxide and anhydride building blocks (a); a single enantiomerically-pure building block (either epoxide or anhydride; b and c); and with racemic epoxide and anhydride monomers (d). As stereoregularity is enhanced, signals in the ^{1}H NMR spectra sharpen, which is illustrated by the conversion of broad signals assigned to the methylene units of the ring-opened epoxide in the racemic polymers (Figure 1, 3.8–4.3 ppm, spectra b–d) to sharp, well-defined multiplet peaks in the polymer prepared from enantiopure (*R*)-BO and (*R*)-CPCA (Figure 1, spectrum a, 4.0 and 4.1 ppm; data for the polymer prepared from (*S*)-BO and (*R*)-CPCA is shown in Figure S2). The differences in the olefinic peaks ~6.1–6.4 ppm in spectra a–d (Figure 1) are similarly striking. Likewise, the ^{13}C{^{1}H} NMR spectra of polyesters prepared from both enantiopure epoxide and anhydride display only two sharp carbonyl singlets, whereas polyesters comprised of racemic monomers exhibit multiple broad signals in the same region. Taken together, the NMR data show a highly-ordered regio- and stereoregular microstructure for poly((*R*)-BO-*alt*-(*R*)-CPCA) compared to polymers derived from racemic monomers.

In addition, several low-intensity signals were observed in the ^{1}H NMR spectra (Figure S5). These could be ascribed to: polymer chain-ends; a decreased regioselectivity in the enchainment of PO or CPCA; formation of low molecular weight oligomers; or post-polymerization epimerization or trans-esterification. The high regiocontrol of the catalyst, showcased by the sharp carbonyl signals in the ^{13}C{^{1}H} NMR spectrum, and the lack of evidence for low molecular weight oligomers in GPC data (Figure S47), suggest that the minor signals are not related to regio-irregularity or oligomer formation. To test for post-polymerization epimerization or trans-esterification, we used tris(cyclohexylmethylamino)cyclopropenium chloride ([CyPr]Cl) as co-catalyst instead of [PPN]Cl, as it is known

that [CyPr]Cl suppresses post-polymerization side-reactions following complete monomer conversion. [63] Copolymerization of (*S*)-PO and (*S*)-CPCA was performed with either [PPN]Cl or [CyPr]Cl, and the ^{1}H NMR spectra of the obtained copolymers were compared (Figure S5). They display identical signals, ruling out post-polymerization side-reactions and suggesting that the low-intensity signals correspond to polymer chain-ends.

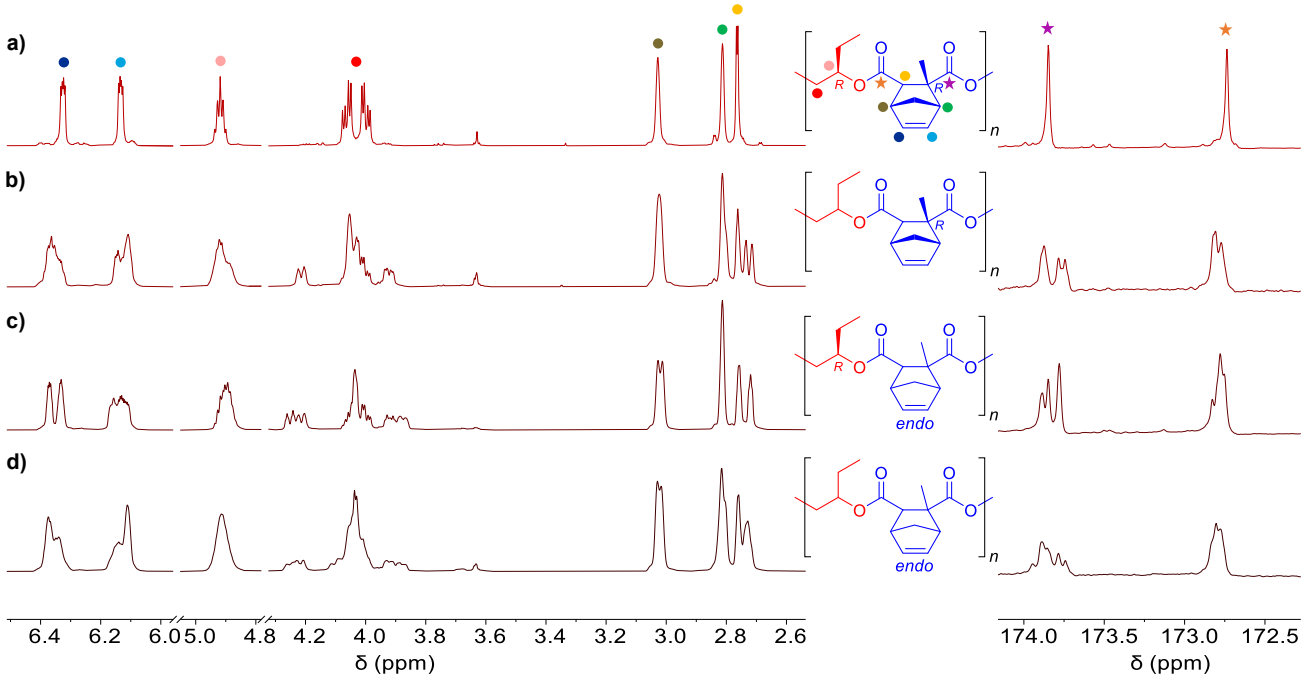

Figure 1. ^{1}H NMR spectra of copolymers prepared with: a) (*R*)-BO and (*R*)-CPCA; b) *rac*-BO and (*R*)-CPCA; c) (*R*)-BO and *rac*-CPCA; d) *rac*-BO and *rac*-CPCA.

Investigation of the thermal properties of the polymers was performed by differential scanning calorimetry (DSC). Poly((*S*)-BO-*alt*-(*S*)-CPCA) and the enantiomeric poly((*R*)-BO-*alt*-(*R*)-CPCA), as well as the polyesters comprising of racemic building blocks, displayed only a T_g between 51 and 57 °C (Table 1, entry 1 and Table S1, entries 1–5) that indicates that they are amorphous. In contrast, poly((*S*)-BO-*alt*-(*R*)-CPCA) and its enantiomer poly((*R*)-BO-*alt*-(*S*)-CPCA) displayed T_m values of 156 °C and 147 °C, respectively, on the first heat only (Table 1, entry 2 and Table S1, entry 6), suggestive of development of crystalline domains in the polymer upon precipitation from solution, situationally. The DSC thermograms (Figure S17–S20) did not exhibit a feature in this temperature regime upon cooling or a T_m on the second heat, indicating no crystallization upon cooling from the melt. We ascribe the slight discrepancy between the T_m values of the enantiomeric polymers to the difference in their molecular weights (8.1 and 6.9 kDa, respectively). The physical appearance of the polymers was also in line with the crystallinity indicated by the DSC data. Namely, the amorphous *R*/*R* and *S*/*S* polymers were lightweight solid foams while the semicrystalline *S*/*R* and *R*/*S* polymers were granular solids (Figure S50). Interestingly, despite the well-defined microstructures exhibited by all polyesters derived from enantiomerically-pure building blocks, only the combination of *S*/*R* (or the enantiomeric *R*/*S*) building blocks displayed situational semicrystallinity.

As in the case of BO-based copolymers, the PO-based *R*/*R* and *S*/*S* copolymers lacked a melting event in their DSC thermograms (Table 1, entry 5, and Table S1, entry 11) and thus are amorphous, while the *S*/*R* and *R*/*S* copolymers showed T_m features indicative of crystallinity. Notably, the T_m values for these PO-based copolymers were dramatically higher than for the corresponding BO-based systems, by 35 °C to 53 °C (Table 1, entries 2 and 6; Table S1, entries 12 and 13). We attribute the higher T_m values for the PO-based copolymers to tighter packing enabled by the less mobile/flexible methyl vs. ethyl side chain. Another difference relative to the BO-based polymers (Figure S27–S30) is the appearance of repetitive melting behavior in the DSC thermograms for the PO-based copolymers, with a crystallization event upon the standard cooling condition, as well as T_m on the second heat, although with slightly lower values than on the first heat. The data thus show that the PO/CPCA polymers have higher crystallinity than their analogous BO/CPCA polymers. Most importantly, the data demonstrate that a transition from an amorphous to a semicrystalline polymer is enabled by a single inversion of a stereocenter along the polymer chain, and that a specific chiral combination of both epoxide and anhydride results in preferential packing, which affects the polymer crystallinity.

To investigate the possible formation of stereocomplexes, equivalent amounts of polymers comprised of building blocks with opposed chiral senses were mixed in DCM and the solvent was allowed to slowly evaporate. The 1:1 mixture of poly((*S*)-BO-*alt*-(*S*)-CPCA) and poly((*R*)-BO-*alt*-(*R*)-CPCA) only displaying a T_g value of 51 °C, between that of the two enantiopure polymer strands (Table 1, entry 3), and thus is not semicrystalline. Similar results were found for the PO/CPCA copolymers (Table 1, entry 7). In contrast,

mixing the situational semicrystalline poly((*S*)-BO-*alt*-(*R*)-CPCA) and poly((*R*)-BO-*alt*-(*S*)-CPCA) copolymers led to an average increase in the T_m of about 15 °C (Table 1, entry 4), suggesting stereocomplexation. Nevertheless, crystallization from the melt was not observed in the DSC thermogram. The *S*/*R* and *R*/*S* stereocomplex of the PO-based polyesters afforded an increase of ca. 22 °C in the T_m on the first heat relative to the enantiopure polymers, and crystallization upon cooling at approximately 173 °C, along with a melting event on the second heating cycle (Table 1, entry 8; Figure S32). The immediate crystallization from the melt was previously noted for other PO-based polyesters, indicating higher crystallinity and more stable interlocked stacking.[45] Notably, the semicrystalline complex is insoluble in THF for GPC analysis, in contrast to the individual polymers which readily dissolve.

Upon subjecting the copolymers to multiple DSC cycles,

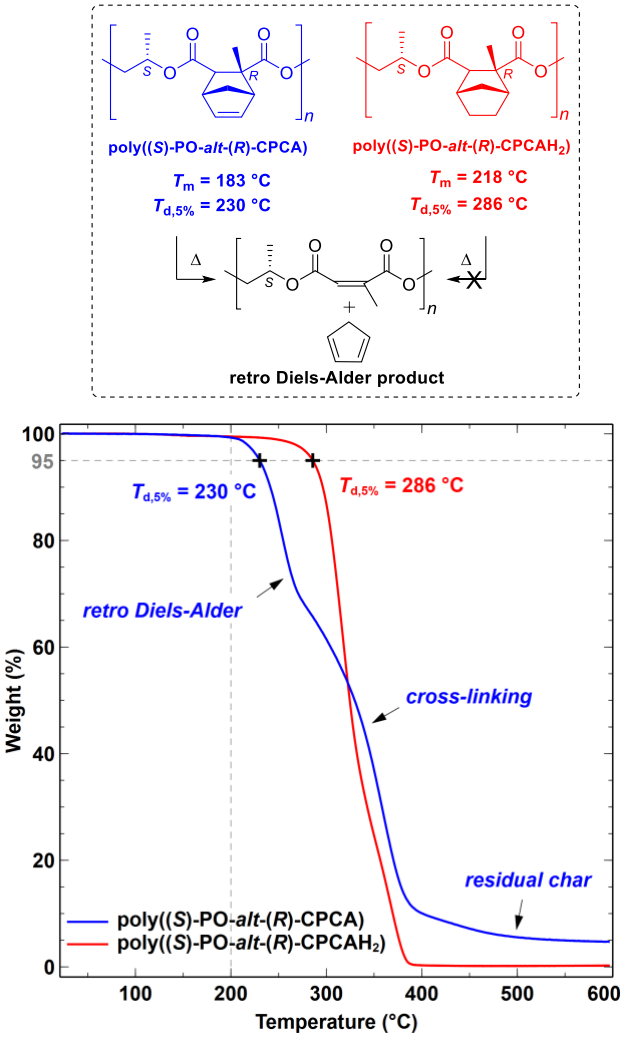

Figure 2. TGA curves of poly((*S*)-PO-*alt*-(*R*)-CPCA) (blue) and poly((*S*)-PO-*alt*-(*R*)-CPCAH$_2$) (red).

we noticed a decrease in their T_g and T_m values. These changes were accompanied by broadening in GPC traces and new signals in ^{1}H NMR spectra (Figures S47 and S48). These data point to a modification in the polyester chemical structure upon heating above the T_m. We performed a series of experiments to elucidate the degradation pathway. First, thermogravimetric analysis (TGA) was used to account for the mass loss upon heating. The TGA curve (Figure 2; blue line) displays a two-step process, with initial degradation ($T_{d,5\%}$) at 230 °C. The remaining mass after the first step correlates well with the expected residual mass (72%) following the removal of a cyclopentadiene unit from the polymer backbone in a *retro* Diels–Alder process. Furthermore, the ^{1}H NMR spectrum of the polymer after heating (Figures S48 and S49) further supports the hypothesis, revealing the formation of new sharp signals at 5.8 and 2.1 ppm, assigned to the double bond proton and methyl in the resulting polymer, poly(propylene citraconate), respectively. Finally, we subjected a sample of a poly((*S*)-PO-*alt*-(*R*)-CPCA) copolymer to heat (260 °C) in a sealed vial for 2 min. and condensed the vapor phase by rapid freezing. A brown polymeric material along with a colorless liquid were obtained, which were separated and analyzed by ^{1}H NMR spectroscopy. The NMR spectrum of the polymer was similar to previously recorded data following polymer degradation, and that of the liquid corresponded to cyclopentadiene (Figure S49). Taken together, the results show that the poly(BO/PO-*alt*-CPCA) systems undergo thermal degradation via a *retro*-Diels–Alder reaction.

Table 2. Polymerization conditions and characterization of poly(PO-*alt*-CPCAH$_2$)

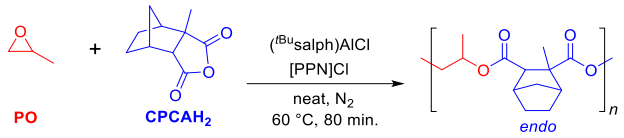

entry[a]	PO/CPCAH$_2$	$M_{n\,GPC}$ (kDa)[b]	$Đ$[b]	T_g (°C)[c]	T_m (°C)[c] 1st	T_m (°C)[c] 2nd	T_c (°C)[c]
1	*R*/*R*	6.7	1.15	74	n.d.	n.d.	n.d.
2	*S*/*R*	8.9	1.15	75	218	218	178
3	*R*/*R* + *S*/*S*[d]	–[e]	–[e]	72	206	n.d.	n.d.
4	*S*/*R* + *R*/*S*[d]	–[e]	–[e]	73	240	238	184

[a] [epoxide]:[CPCA]:[cat.]:[PPNCl] = 500:100:1:1. [epoxide] = 3.8 mmol. [b] Determined by GPC in THF, calibrated with polystyrene standards. [c] Determined by DSC. Reported T_g values are from second heat, T_m values are from first heat and second heat, and T_c values are from the first cool. [d] 1:1 mixture of enantiomeric polymers. [e] Not determined because of poor solubility. n.d. = none detected.

To avoid the degradation of the polyesters with similar T_m and T_d values, the enantiopure CPCA monomers were hydrogenated to the corresponding CPCAH$_2$ anhydrides in high yield (90%, Scheme 2; g), and subsequently employed as monomers for ROCOP with PO. The copolymers were obtained in similar yields to their CPCA-based analogues and displayed corresponding M_n and $Đ$ values (Table 2 and Table S1). ^{1}H NMR spectra of the copolymers confirm the retention of high regiocontrol in the polymerization process as well (Figure S6). Interestingly, DSC measurements display an increase in both the T_g and the T_m of the copolymers relative to their CPCA-based analogues (Table 2, entries 1 and 2). Furthermore, poly((*S*)-PO-*alt*-(*R*)-

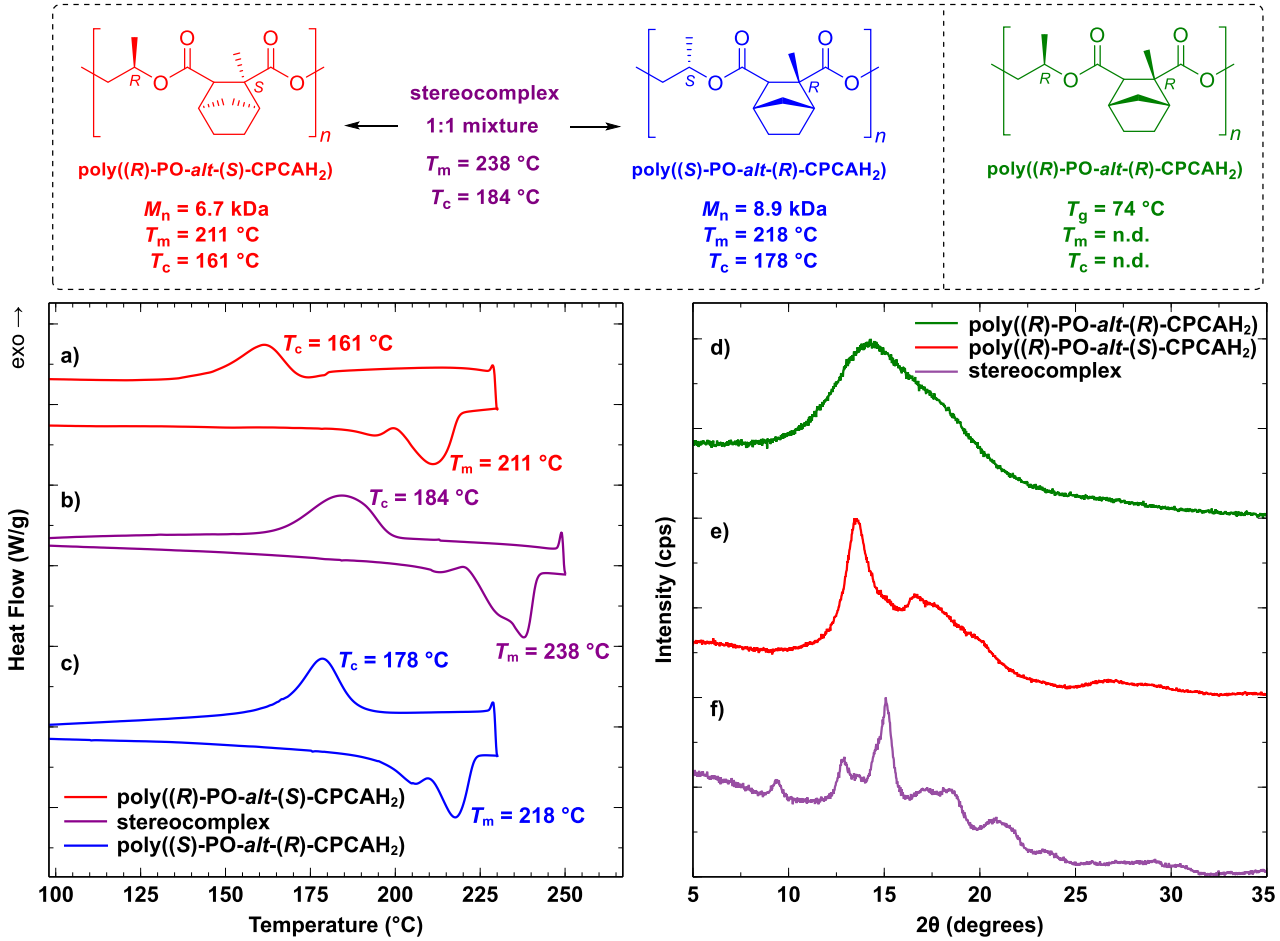

Figure 3. DSC thermograms (left) and PXRD spectra (right) of poly(PO-*alt*-CPCAH$_2$): poly((*R*)-PO-*alt*-(*S*)-CPCAH$_2$) (red); poly((*S*)-PO-*alt*-(*R*)-CPCAH$_2$) (blue); their stereocomplex (purple); and poly((*R*)-PO-*alt*-(*R*)-CPCAH$_2$) (green).

CPCAH$_2$) and poly((*R*)-PO-*alt*-(*S*)-CPCAH$_2$) not only crystallize upon cooling from the melt, but also exhibit an almost identical T_m during the second heat, in contrast to the CPCA-based polyesters. TGA analysis was used to validate the higher stability of the CPCAH$_2$-based polymers, compared to CPCA-based polymers, at elevated temperatures. Figure 2 shows that both poly((*S*)-PO-*alt*-(*R*)-CPCAH$_2$) and poly((*S*)-PO-*alt*-(*R*)-CPCA) are thermally-stable under 200 °C. However, the $T_{d,5\%}$ of the former is much higher compared to the CPCA-based copolymer, 286 °C vs. 230 °C. The CPCAH$_2$-based polymer exhibits a straightforward one-step degradation, and is completely degraded at approximately 380 °C. Conversely, the CPCA-based polymer displays a two-step degradation pattern, with initial degradation at a relatively lower temperature due to the release of cyclopentadiene during the first stage (*vide supra*). We postulate that in this case, the residual polymer backbone has an alkene functionality, which may undergo cross-linking under heat, shifting the second step degradation to a higher temperature (which starts to cross over that of the CPCAH$_2$-based polymer at about 325 °C) and making complete degradation harder to achieve.

Similar to the CPCA-based polyesters, stereocomplexation by mixing semicrystalline poly((*S*)-PO-*alt*-(*R*)-CPCAH$_2$) and poly((*R*)-PO-*alt*-(*S*)-CPCAH$_2$) in DCM leads to an approximate 20 °C increase in the T_m with respect to the enantiopure polymers, resulting in a fairly high melting temperature of 238 °C, and a crystallization temperature of 184 °C (Figure 3a–3c; Table 2, entry 4). The stereocomplex T_m is considerably higher than that of isotactic polypropylene (*i*PP; 171 °C) and close to polyethylene terephthalate (PET; 250 °C).[64,65] Interestingly, mixing the amorphous poly((*R*)-PO-*alt*-(*R*)-CPCAH$_2$) and poly((*S*)-PO-*alt*-(*S*)-CPCAH$_2$) polyesters results in the formation of a semicrystalline stereocomplex for the first time in these polymer series, with a T_m of 206 °C observed situationally only on the first heat, probably due to the high backbone rigidity and tight packing regardless of the less ideal *S*/*S* or *R*/*R* stereocenter combination (Figure S43; Table 2, entry 3). We conclude that for all three polymer series, the *S*/*R* and *R*/*S* chirality combination affords crystallinity and stereocomplexation, with the poly(PO-*alt*-CPCAH$_2$) series displaying the highest crystallinity.

Powder X-Ray Diffraction (PXRD) was employed to further study the crystallinity of the poly(PO-*alt*-CPCAH$_2$) copolymers. Poly((*R*)-PO-*alt*-(*R*)-CPCAH$_2$) exhibits one broad diffraction signal at 14.3° (Figure 3d), whereas poly((*R*)-PO-*alt*-(*S*)-CPCAH$_2$) displays two distinct crystalline diffraction peaks at 13.6° and 16.6° (Figure 3e). The increasing peak sharpness showcases the higher crystallinity. The mixture of poly((*R*)-PO-*alt*-(*S*)-CPCAH$_2$) and poly((*S*)-PO-*alt*-(*R*)-CPCAH$_2$) exhibits new intense

crystalline diffraction signals at 12.9° and 15.1°, along with four minor signals at 9.4°, 17.2°, 18.1°, and 20.9° (Figure 3f). The different diffraction patterns prove the formation of new crystalline domains, consistent with the formation of a stereocomplex.

Conclusions

In this work we describe the first fundamental study of the relationship between the chirality of both epoxide and anhydride and the crystallinity of the resulting copolymers and their stereocomplexes. We successfully resolved racemic CPCA into its two enantiomers, and synthesized a series of their highly regio- and stereoregular copolymers with BO and PO by ROCOP, using the highly regioselective salph-Al catalyst. The enantiopure poly(BO-*alt*-CPCA) and poly(PO-*alt*-CPCA) copolymers display stereocomplexation behavior, which is derived from a specific combination of homochiral polymer constituents. Following monomer structural optimization, we were able to improve the resulting polymer crystallinity and thermal stability. The poly(PO-*alt*-CPCAH$_2$) copolymers exhibit an increase of 20 °C in the T_m following stereocomplexation, providing an aliphatic polyester stereocomplex with a T_m as high as 238 °C. Future work will be focused on the development of catalysts for enantioselective ROCOP, to allow in situ stereocomplexation, as well as the investigation of polymerizations using additional bio-sourced enantiomerically-pure anhydrides to obtain polyesters with high melting temperatures.

AUTHOR INFORMATION

Corresponding Authors

William B. Tolman – Department of Chemistry, Washington University in St. Louis, One Brookings Hall, Campus Box 1134, St. Louis, MO 63130-4899, United States; orcid.org/0000-0002-2243-6409; Email: wbtolman@wustl.edu

Geoffrey W. Coates – Department of Chemistry and Chemical Biology, Baker Laboratory, Cornell University, Ithaca, New York 14853-1301, United States; orcid.org/0000-0002-3400-2552; Email: coates@cornell.edu

Authors

Yanay Popowski – Department of Chemistry, Washington University in St. Louis, One Brookings Hall, Campus Box 1134, St. Louis, MO 63130-4899, United States; orcid.org/0000-0003-1569-0035

Yiye Lu – Department of Chemistry and Chemical Biology, Baker Laboratory, Cornell University, Ithaca, New York 14853-1301, United States; orcid.org/0000-0002-6702-1258

Complete contact information is available at: http://pubs.acs.org.

Author Contributions

‡Y. P. and Y. L. contributed equally to this work.

Notes

The authors declare no competing financial interest.

SUPPORTING INFORMATION

Descriptions of methods and procedures; spectroscopic and other characterization data.

ACKNOWLEDGMENT

This research was supported by the Center for Sustainable Polymers, a National Science Foundation (NSF) Center for Chemical Innovation (CHE-1901635) and Cornell University. The authors thank Dr. Chenyue Sun for assistance with PXRD, and Dr. Minsoo Ju for help with chiral HPLC. This work made use of the Cornell Center for Materials Research Shared Facilities which are supported through the NSF MRSEC program (DMR-1719875).

REFERENCES

(1) Gross, R. A.; Kalra, B. Biodegradable Polymers for the Environment. *Science* **2002**, *297*, 803–807.

(2) Ikada, Y.; Tsuji, H. Biodegradable polyesters for medical and ecological applications. *Macromol. Rapid Commun.* **2000**, *21*, 117–132.

(3) Ragauskas, A. J.; Williams, C. K.; Davison, B. H.; Britovsek, G.; Cairney, J.; Eckert, C. A.; Frederick, W. J.; Hallett, J. P.; Leak, D. J.; Liotta, C. L.; Mielenz, J. R.; Murphy, R.; Templer, R.; Tschaplinski, T. The Path Forward for Biofuels and Biomaterials. *Science* **2006**, *311*, 484–489.

(4) Vert, M. Aliphatic Polyesters: Great Degradable Polymers That Cannot Do Everything. *Biomacromolecules* **2005**, *6*, 538–546.

(5) Sanford, M. J.; Van Zee, N. J.; Coates, G. W. Reversible-deactivation anionic alternating ring-opening copolymerization of epoxides and cyclic anhydrides: access to orthogonally functionalizable multiblock aliphatic polyesters. *Chem. Sci.* **2018**, *9*, 134–142.

(6) Longo, J. M.; Sanford, M. J.; Coates, G. W. Ring-Opening Copolymerization of Epoxides and Cyclic Anhydrides with Discrete Metal Complexes: Structure–Property Relationships. *Chem. Rev.* **2016**, *116*, 15167–15197.

(7) Van Zee, N. J.; Coates, G. W. Alternating Copolymerization of Propylene Oxide with Biorenewable Terpene-Based Cyclic Anhydrides: A Sustainable Route to Aliphatic Polyesters with High Glass Transition Temperatures. *Angew. Chem. Int. Ed.* **2015**, *54*, 2665–2668.

(8) Sanford, M. J.; Peña Carrodeguas, L.; Van Zee, N. J.; Kleij, A. W.; Coates, G. W. Alternating Copolymerization of Propylene Oxide and Cyclohexene Oxide with Tricyclic Anhydrides: Access to Partially Renewable Aliphatic Polyesters with High Glass Transition Temperatures. *Macromolecules* **2016**, *49*, 6394–6400.

(9) Robert, C.; de Montigny, F.; Thomas, C. M. Tandem synthesis of alternating polyesters from renewable resources. *Nat. Commun.* **2011**, *2*, 586.

(10) Worch, J. C.; Prydderch, H.; Jimaja, S.; Bexis, P.; Becker, M. L.; Dove, A. P. Stereochemical enhancement of polymer properties. *Nat. Rev. Chem.* **2019**, *3*, 514–535.

(11) Tang, X.; Westlie, A. H.; Watson, E. M.; Chen, E. Y.-X. Stereosequenced crystalline polyhydroxyalkanoates from diastereomeric monomer mixtures. *Science* **2019**, *366*, 754–758.

(12) Liu, Y.; Ren, W.-M.; Wang, M.; Liu, C.; Lu, X.-B. Crystalline Stereocomplexed Polycarbonates: Hydrogen-Bond-Driven Interlocked Orderly Assembly of the Opposite Enantiomers. *Angew. Chem. Int. Ed.* **2015**, *54*, 2241–2244.

(13) Tutoni, G.; Becker, M. L. Underexplored Stereocomplex Polymeric Scaffolds with Improved Thermal and Mechanical Properties. *Macromolecules* **2020**, *53*, 10303–10314.

(14) Bertin, A. Emergence of Polymer Stereocomplexes for Biomedical Applications. *Macromol. Chem. Phys.* **2012**, *213*, 2329–2352.

(15) Tsuji, H. Poly(lactide) Stereocomplexes: Formation, Structure, Properties, Degradation, and Applications. *Macromol. Biosci.* **2005**, *5*, 569–597.

(16) Brizzolara, D.; Cantow, H.-J.; Diederichs, K.; Keller, E.; Domb, A. J. Mechanism of the Stereocomplex Formation between Enantiomeric Poly(lactide)s. *Macromolecules* **1996**, *29*, 191–197.

(17) Serizawa, T.; Hamada, K.-i.; Kitayama, T.; Fujimoto, N.; Hatada, K.; Akashi, M. Stepwise Stereocomplex Assembly of Stereoregular Poly(methyl methacrylate)s on a Substrate. *J. Am. Chem. Soc.* **2000**, *122*, 1891–1899.

(18) Kida, T.; Mouri, M.; Akashi, M. Fabrication of Hollow Capsules Composed of Poly(methyl methacrylate) Stereocomplex Films. *Angew. Chem. Int. Ed.* **2006**, *45*, 7534–7536.

(19) Kawauchi, T.; Kitaura, A.; Kumaki, J.; Kusanagi, H.; Yashima, E. Helix-Sense-Controlled Synthesis of Optically Active Poly(methyl methacrylate) Stereocomplexes. *J. Am. Chem. Soc.* **2008**, *130*, 11889–11891.

(20) Kumaki, J.; Kawauchi, T.; Okoshi, K.; Kusanagi, H.; Yashima, E. Supramolecular Helical Structure of the Stereocomplex Composed of Complementary Isotactic and Syndiotactic Poly(methyl methacrylate)s as Revealed by Atomic Force Microscopy. *Angew. Chem. Int. Ed.* **2007**, *46*, 5348–5351.

(21) Goh, T. K.; Tan, J. F.; Guntari, S. N.; Satoh, K.; Blencowe, A.; Kamigaito, M.; Qiao, G. G. Nano-to-Macroscale Poly(methyl methacrylate) Stereocomplex Assemblies. *Angew. Chem. Int. Ed.* **2009**, *48*, 8707–8711.

(22) Wang, X.; Hong, M. Precise Control of Molecular Weight and Stereospecificity in Lewis Pair Polymerization of Semifluorinated Methacrylates: Mechanistic Studies and Stereocomplex Formation. *Macromolecules* **2020**, *53*, 4659–4669.

(23) Nakano, K.; Hashimoto, S.; Nakamura, M.; Kamada, T.; Nozaki, K. Stereocomplex of Poly(propylene carbonate): Synthesis of Stereogradient Poly(propylene carbonate) by Regio- and Enantioselective Copolymerization of Propylene Oxide with Carbon Dioxide. *Angew. Chem. Int. Ed.* **2011**, *50*, 4868–4871.

(24) Liu, Y.; Wang, M.; Ren, W.-M.; Xu, Y.-C.; Lu, X.-B. Crystalline Hetero-Stereocomplexed Polycarbonates Produced from Amorphous Opposite Enantiomers Having Different Chemical Structures. *Angew. Chem. Int. Ed.* **2015**, *54*, 7042–7046.

(25) Liu, Y.; Fang, L.-M.; Ren, B.-H.; Lu, X.-B. Asymmetric Alternating Copolymerization of CO_2 with *meso*-Epoxides: Ring Size Effects of Epoxides on Reactivity, Enantioselectivity, Crystallization, and Degradation. *Macromolecules* **2020**, *53*, 2912–2918.

(26) Ren, W.-M.; Yue, T.-J.; Zhang, X.; Gu, G.-G.; Liu, Y.; Lu, X.-B. Stereoregular CO_2 Copolymers from Epoxides with an Electron-Withdrawing Group: Crystallization and Unexpected Stereocomplexation. *Macromolecules* **2017**, *50*, 7062–7069.

(27) Auriemma, F.; De Rosa, C.; Di Caprio, M. R.; Di Girolamo, R.; Ellis, W. C.; Coates, G. W. Stereocomplexed Poly(Limonene Carbonate): A Unique Example of the Cocrystallization of Amorphous Enantiomeric Polymers. *Angew. Chem. Int. Ed.* **2015**, *54*, 1215–1218.

(28) Auriemma, F.; De Rosa, C.; Di Caprio, M. R.; Di Girolamo, R.; Coates, G. W. Crystallization of Alternating Limonene Oxide/Carbon Dioxide Copolymers: Determination of the Crystal Structure of Stereocomplex Poly(limonene carbonate). *Macromolecules* **2015**, *48*, 2534–2550.

(29) DeRosa, C. A.; Luke, A. M.; Anderson, K.; Reineke, T. M.; Tolman, W. B.; Bates, F. S.; Hillmyer, M. A. Regioregular Polymers from Biobased (*R*)-1,3-Butylene Carbonate. *Macromolecules* **2021**, *54*, 5974–5984.

(30) Tsuji, H.; Okumura, A. Stereocomplex Formation between Enantiomeric Substituted Poly(lactide)s: Blends of Poly[(*S*)-2-hydroxybutyrate] and Poly[(*R*)-2-hydroxybutyrate]. *Macromolecules* **2009**, *42*, 7263–7266.

(31) Andersson, S. R.; Hakkarainen, M.; Albertsson, A.-C. Stereocomplexation between PLA-like substituted oligomers and the influence on the hydrolytic degradation. *Polymer* **2013**, *54*, 4105–4111.

(32) Tsuji, H.; Nakayama, K.; Arakawa, Y. Synthesis and stereocomplex formation of enantiomeric alternating copolymers with two types of chiral centers, poly(lactic acid-*alt*-2-hydroxybutanoic acid)s. *RSC Adv.* **2020**, *10*, 39000–39007.

(33) McGuire, T. M.; Bowles, J.; Deane, E.; Farrar, E. H. E.; Grayson, M. N.; Buchard, A. Control of Crystallinity and Stereocomplexation of Synthetic Carbohydrate Polymers from D- and L-Xylose *Angew. Chem. Int. Ed.* **2021**, *60*, 4524–4528.

(34) Siriwardane, D. A.; Kulikov, O.; Rokhlenko, Y.; Perananthan, S.; Novak, B. M. Stereocomplexation of Helical Polycarbodiimides Synthesized from Achiral Monomers Bearing Isopropyl Pendants. *Macromolecules* **2017**, *50*, 9162–9172.

(35) Zhu, J.-B.; Watson, E. M.; Tang, J.; Chen, E. Y.-X. A synthetic polymer system with repeatable chemical recyclability. *Science* **2018**, *360*, 398–403.

(36) Zhu, J.-B.; Chen, E. Y.-X. Catalyst-Sidearm-Induced Stereoselectivity Switching in Polymerization of a Racemic Lactone for Stereocomplexed Crystalline Polymer with a Circular Life Cycle. *Angew. Chem. Int. Ed.* **2019**, *58*, 1178–1182.

(37) Jia, Z.; Jiang, J.; Zhang, X.; Cui, Y.; Chen, Z.; Pan, X.; Wu, J. Isotactic-Alternating, Heterotactic-Alternating, and ABAA-Type Sequence-Controlled Copolyester Syntheses via Highly Stereoselective and Regioselective Ring-Opening Polymerization of Cyclic Diesters. *J. Am. Chem. Soc.* **2021**, *143*, 4421–4432.

(38) Jiang, J.; Cui, Y.; Lu, Y.; Zhang, B.; Pan, X.; Wu, J. Weak Lewis Pairs as Catalysts for Highly Isoselective Ring-Opening Polymerization of Epimerically Labile *rac*-*O*-Carboxyanhydride of Mandelic Acid. *Macromolecules* **2020**, *53*, 946–955.

(39) Jiang, J.; Cui, Y.; Jia, Z.; Pan, X.; Wu, J. Living Polymerization of Chiral *O*-Carboxyanhydride of Mandelic Acid and Precise Stereoblock Copolymer Syntheses Using Highly Active OOO-Tridentate Bis(phenolate) Zinc Complexes. *Macromolecules* **2021**, *54*, 2232–2241.

(40) Li, M.; Tao, Y.; Tang, J.; Wang, Y.; Zhang, X.; Tao, Y.; Wang, X. Synergetic Organocatalysis for Eliminating Epimerization in Ring-Opening Polymerizations Enables Synthesis of Stereoregular Isotactic Polyester. *J. Am. Chem. Soc.* **2019**, *141*, 281–289.

(41) Wang, Y.; Xu, T.-Q. Topology-Controlled Ring-Opening Polymerization of *O*-Carboxyanhydride. *Macromolecules* **2020**, *53*, 8829–8836.

(42) Bandelli, D.; Alex, J.; Weber, C.; Schubert, U. S. Polyester Stereocomplexes Beyond PLA: Could Synthetic Opportunities Revolutionize Established Material Blending? *Macromol. Rapid Commun.* **2020**, *41*, 1900560.

(43) Tu, Y.-M.; Wang, X.-M.; Yang, X.; Fan, H.-Z.; Gong, F.-L.; Cai, Z.; Zhu, J.-B. Biobased High-Performance Aromatic–Aliphatic Polyesters with Complete Recyclability. *J. Am. Chem. Soc.* **2021**, *143*, 20591–20597.

(44) Xia, B.; Zhang, Y.; Zhu, Q.; Lin, X.; Wu, Q. Enzymatic Synthesis and Stereocomplex Formation of Chiral Polyester Containing Long-Chain Aliphatic Alcohol Backbone. *Biomacromolecules* **2019**, *20*, 3584–3591.

(45) Fraschini, C.; Pennors, A.; Prud'homme, R. E. Stereocomplex formation between enantiomeric poly(*α*-methyl-*α*-ethyl-*β*-propiolactones): Effect of molecular weight. *J. Polym. Sci., Part B: Polym. Phys.* **2007**, *45*, 2380–2389.

(46) Zheng, Y.; Pan, P. Crystallization of biodegradable and biobased polyesters: Polymorphism, cocrystallization, and structure-property relationship. *Prog. Polym. Sci.* **2020**, *109*, 101291.

(47) Longo, J. M.; DiCiccio, A. M.; Coates, G. W. Poly(propylene succinate): A New Polymer Stereocomplex. *J. Am. Chem. Soc.* **2014**, *136*, 15897–15900.

(48) Wan, Z.-Q.; Longo, J. M.; Liang, L.-X.; Chen, H.-Y.; Hou, G.-J.; Yang, S.; Zhang, W.-P.; Coates, G. W.; Lu, X.-B. Comprehensive

Understanding of Polyester Stereocomplexation. *J. Am. Chem. Soc.* **2019**, *141*, 14780–14787.

(49) Li, J.; Wang, M.-W.; Liu, Y.; Ren, W.-M.; Lu, X.-B. Photoinduced Reversible Semicrystalline-to-Amorphous State Transitions of Stereoregular Azopolyesters. *Angew. Chem. Int. Ed.* **2021**, *60*, 17898–17903.

(50) Li, J.; Ren, B.-H.; Chen, S.-Y.; He, G.-H.; Liu, Y.; Ren, W.-M.; Zhou, H.; Lu, X.-B. Development of Highly Enantioselective Catalysts for Asymmetric Copolymerization of *meso*-Epoxides and Cyclic Anhydrides: Subtle Modification Resulting in Superior Enantioselectivity. *ACS Catal.* **2019**, *9*, 1915–1922.

(51) Han, B.; Zhang, L.; Liu, B.; Dong, X.; Kim, I.; Duan, Z.; Theato, P. Controllable Synthesis of Stereoregular Polyesters by Organocatalytic Alternating Copolymerizations of Cyclohexene Oxide and Norbornene Anhydrides. *Macromolecules* **2015**, *48*, 3431–3437.

(52) Han, B.; Zhang, L.; Yang, M.; Liu, B.; Dong, X.; Theato, P. Highly *Cis*/*Trans*-Stereoselective (ONSO)CrCl-Catalyzed Ring-Opening Copolymerization of Norbornene Anhydrides and Epoxides. *Macromolecules*, **2016**, *49*, 6232–6239.

(53) Ji, H.-Y.; Chen, X.-L.; Wang, B.; Pan, L.; Li, Y.-S. Metal-free, regioselective and stereoregular alternating copolymerization of monosubstituted epoxides and tricyclic anhydrides. *Green Chem*., **2018**, *20*, 3963–3973.

(54) Wan, Z.-Q.; Ren, W.-M.; Yang, S.; Li, M.-R.; Gu, G.-G.; Lu, X.-B. Reversible Transformation between Amorphous and Crystalline States of Unsaturated Polyesters by *Cis*–*Trans* Isomerization. *Angew. Chem. Int. Ed.* **2019**, *58*, 17636–17640.

(55) Hu, L.; Zhang, X.; Cao, X.; Chen, D.; Sun, Y.; Zhang, C.; Zhang, X. Alternating Copolymerization of Isobutylene Oxide and Cyclic Anhydrides: A New Route to Semicrystalline Polyesters. *Macromolecules* **2021**, *54*, 6182–6190.

(56) Popowski, Y.; Moreno, J. J.; Nichols, A. W.; Hooe, S. L.; Bouchey, C. J.; Rath, N. P.; Machan, C. W.; Tolman, W. B. Mechanistic insight into initiation and regioselectivity in the copolymerization of epoxides and anhydrides by Al complexes. *Chem. Commun.* **2020**, *56*, 14027–14030.

(57) Schneider, K. J.; Williams, J. D. Sodium Sulfide Catalyzed Isomerization of Itaconic Anhydride to Citraconic Anhydride. *Curr. Org. Chem.* **2011**, *15*, 2893–2896.

(58) Robert, C.; de Montigny, F.; Thomas, C. M. Facile and Efficient Synthesis of Cyclic Anhydrides from Dicarboxylic Acids. *ACS Catal.* **2014**, *4*, 3586–3589.

(59) Okabe, M.; Lies, D.; Kanamasa, S.; Park, E. Y. Biotechnological production of itaconic acid and its biosynthesis in Aspergillus terreus. *Appl. Microbiol. Biotechnol.* **2009**, *84*, 597–606.

(60) Polonski, T.; Milewska, M. J.; Gdaniec, M.; Gilski, M. Molecular geometry and circular dichroism spectra of bicyclo[2.2.1]heptane-2,3-dicarboxylic anhydrides and imides. *J. Org. Chem.* **1993**, *58*, 3134–3139.

(61) Fieser, M. E.; Sanford, M. J.; Mitchell, L. A.; Dunbar, C. R.; Mandal, M.; Van Zee, N. J.; Urness, D. M.; Cramer, C. J.; Coates, G. W.; Tolman, W. B. Mechanistic Insights into the Alternating Copolymerization of Epoxides and Cyclic Anhydrides Using a (Salph)AlCl and Iminium Salt Catalytic System. *J. Am. Chem. Soc.* **2017**, *139*, 15222–15231.

(62) Lidston, C. A. L.; Abel, B. A.; Coates, G. W. Bifunctional Catalysis Prevents Inhibition in Reversible-Deactivation Ring-Opening Copolymerizations of Epoxides and Cyclic Anhydrides. *J. Am. Chem. Soc.* **2020**, *142*, 20161–20169.

(63) Abel, B. A.; Lidston, C. A. L.; Coates, G. W. Mechanism-Inspired Design of Bifunctional Catalysts for the Alternating Ring-Opening Copolymerization of Epoxides and Cyclic Anhydrides. *J. Am. Chem. Soc.* **2019**, *141*, 12760–12769.

(64) Ballara, A.; Verdu, J. Physical aspects of the hydrolysis of polyethylene terephthalate. *Polym. Degrad. Stab.* **1989**, *26*, 361–374.

(65) Asgarpour, M.; Bakir, F.; Khelladi, S.; Khavandi, A.; Tcharkhtchi, A. Characterization and modeling of sintering of polymer particles. *J. Appl. Polym. Sci.* **2011**, *119*, 2784–2792.

Table of Contents Graphic